Responses to Reviewer:

General comments*: This paper proposes a method for calculating rainfall thresholds for rainfall-induced landslides using the Multilayer Perceptron regression method and the feasibility of this method has been verified. In addition, the authors use a large amount of data and various data-driven modeling techniques. The research results have practical significance for the early warning and prevention of rainfall-induced landslides. It is recommended that the paper be published after revisions, addressing the following comments:*

Response: We thank you for your recommendation and valuable comments that have ultimately improved this manuscript. We greatly appreciate you for the very extensive and thoughtful review of the manuscript. According to your comments, we have made point by point corrections which we hope meet with your approval.

Point by point responses to the nine comments:

1. Comment*: The originality of the study is not prominently highlighted in the abstract. It is recommended to enhance this aspect.*

Response: Thank you for pointing this out. We understand the concern regarding the lack of emphasis on the originality of the study in the abstract. Based on your suggestion, we have revised the abstract to highlight the originality of our research. The revised abstract can be found in lines 6-18 (in red font).

Abstract. Rainfall is intrinsically connected to the incidence of landslide catastrophes.

Exploring the ideal rainfall threshold model (RTM) for an area to determine the rainfall warning level (RWL) for daily landslide hazard warning (LHW) is critical for precise prevention and management of local landslides. In this paper, we propose a novel approach using multilayer perceptron (MLP) regression to calculate rainfall thresholds for 453 rainfall-induced landslides. This is the first study to integrate MLP and ordinary least squares (OLS) methods to determine the optimal RTM for distinct subregions, which were divided based on topography and climate conditions. Additionally, we introduce an innovative application of a three-dimensional convolutional neural network (3D-CNN) model to predict landslide susceptibility (LS) with higher accuracy. Finally, we develop a comprehensive methodology to overlay daily RWL with LS predictions using a superposition matrix, providing daily LHW results for the study area. The study's findings are: (1) The optimal RTMs and calculation methods vary across different subregions, highlighting the necessity of tailored approaches. (2) The 3D-CNN model significantly enhances LS prediction accuracy. (3) The daily LHW was validated using anticipated rainfall data for July 19, 2020, demonstrating the reliability of the LHW results and RTM. This study offers a significant advancement in the precise prediction and management of landslide hazards through innovative modeling techniques.

2. *Comment*: *The use of the Multilayer Perceptron (MLP) for analyzing rainfall thresholds is a commendable innovation. However, since this method has been widely used in other fields, it would suffice to mention it with appropriate references. The MLP framework in Figure 1 is relatively simple and takes up significant space; consider removing it.*

Response: We completely agree with your suggestion. The Multilayer Perceptron (MLP) is a significant model in machine learning and has been widely applied in various research fields by scholars both domestically and internationally. Given that the description of the MLP framework occupies considerable space, we have removed the related basic description and the framework diagram from the revised manuscript.

*3. **Comment**: Given the length of the article and the complexity of the methods and procedures involved, it is suggested that the authors create a flowchart to further elucidate the methodological steps.*

Response: Thank you for bringing this to our attention. We understand your concern regarding the complexity of the content and the lack of a flowchart. To more clearly illustrate the methods and steps involved in the article, we have created a flowchart and included it in the revised manuscript (lines 71-73, in red font).

The flowchart for the study is shown in Fig. 1.

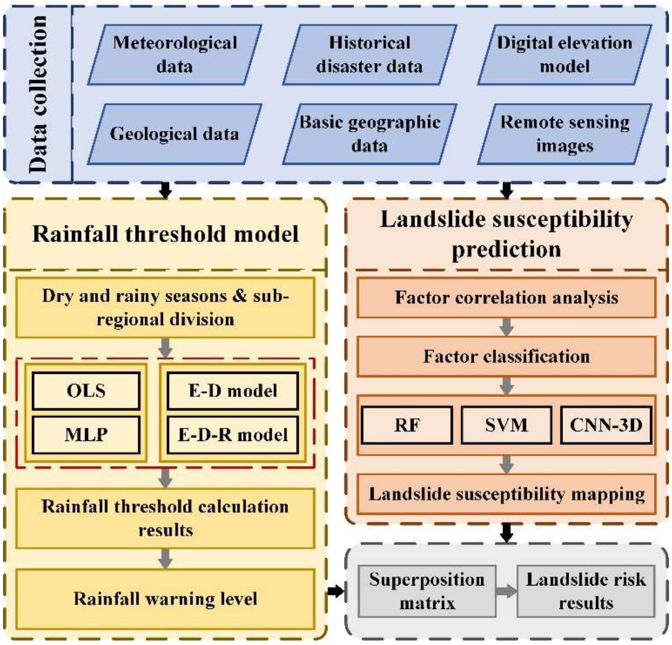

Figure 1. Flowchart of this study.

*4. **Comment**: The paper mentions dividing the study area based on topography and climate, followed by partial merging based on the number of historical disasters. It is suggested to include the final regional division results in Figure 4* *to avoid any ambiguity.*

Response: Your feedback is greatly appreciated and has been very helpful for improving our work. We agree with your suggestion; the absence of the final merged regional division in Figure 4 may cause confusion for readers. Therefore, we have added black outlines and labels to show the final regional divisions in the figure. Additionally, following your seventh suggestion, we have combined Figure 6 with Figure 4. The revised content can be found in lines 147-149 (in red font).

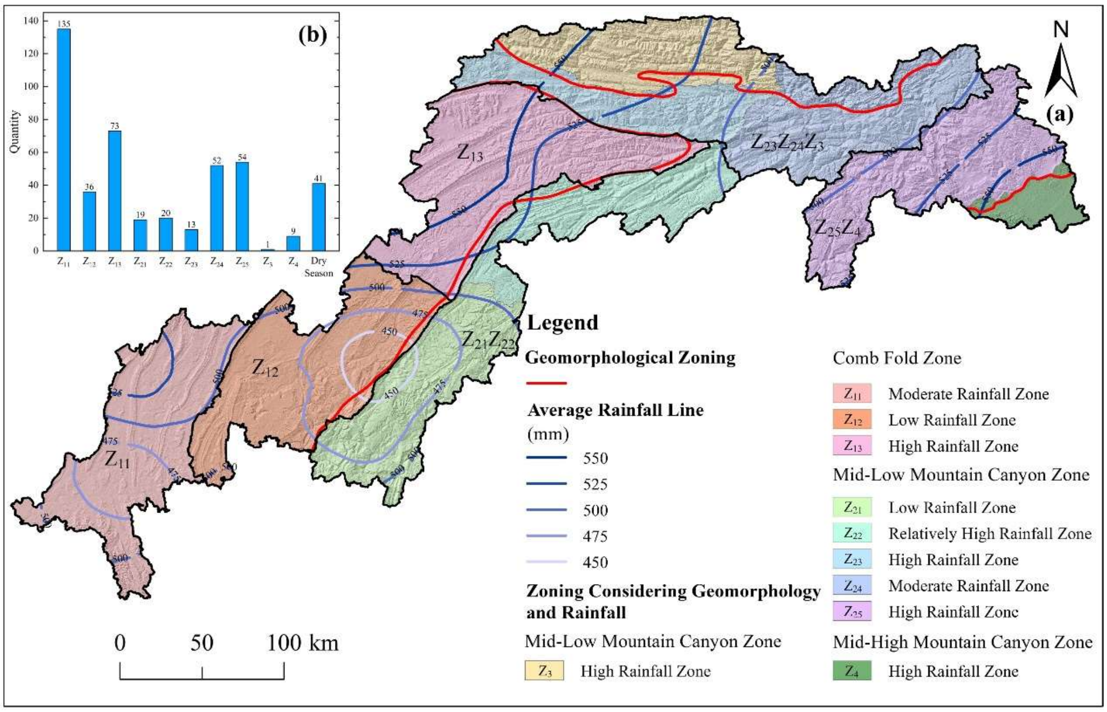

Figure 4: Zoning map of the study area. (a) Schematic diagram of the sub-region merger; (b) The number of historical landslide hazard sites in each sub-region.

5. Comment*: In Table 6, the categories of slope structures are represented by A-H, which is unclear and it is recommended to change them to professional terms.*

Response: Thank you for pointing this out. As you mentioned, using A-H to represent different slope structures may be misleading to readers. We have revised the categories of slope structures in Tables 6 and 7 using professional terminology. The revised content can be found in lines 271 and 295 (in red font).

Table 6: Classification of slope structure types and percentage of each type in the study area.

Class	Relationship between α, β, γ and σ	Area (%)
Nearly horizontal slope	α≤5°	1.720
Over-dip slope	α>5°, |γ-β|∈[0°, 30°) or |γ-β|∈[330°, 360°), σ>α	5.127
Flat-dip slope	α>5°, |γ-β|∈[0°, 30°) or |γ-β|∈[330°, 360°), σ=α	0.000
Under-dip slope	α>5°, |γ-β|∈[0°, 30°) or |γ-β|∈[330°, 360°), σ<α	13.581
Dip-oblique slope	α>5°, |γ-β|∈[30°, 60°) or |γ-β|∈[300°, 330°)	17.559
Transverse slope	α>5°, |γ-β|∈60°, 120°) or |γ-β|∈[240°, 300°)	32.066
Anticlinal-oblique slope	α>5°, |γ-β|∈[120°, 150°) or |γ-β|∈[210°, 240°)	15.089
Anticlinal slope	α>5°, |γ-β|∈[150°, 210°)	14.857

6. Comment*: In Table 7, the units of some landslide susceptibility factors are given, but the units for factors such as road density are missing.*

Response: Thank you for bringing this to our attention. We apologize for the omission of units for landslide susceptibility factors such as road density. In the revised manuscript, we have included the missing units (line 295, in red font).

Table 7: Classification of landslide inducing factors (only the revised part is shown).

Predisposing Factor	Classification Criteria	Code
Road Density (km/km^2)	[0,0.5]	d
	(0.5,1.2]	
	(1.2,2.5]	
	(2.5,5.0]	
	>5.0	
Tectonic Density (km/km^2)	[0,0.03]	f
	(0.03,0.12]	
	(0.12,0.24]	

	(0.24,0.38]	
	>0.38	
Curvature (m^{-1})	≤-3	i
	(-3,-1]	
	(-1,0]	
	(0,1]	
	>1	
Slope Structure	Nearly horizontal slope	k
	Over-dip slope	
	Under-dip slope	
	Dip-oblique slope	
	Transverse slope	
	Anticlinal-oblique slope	
	Anticlinal slope	

7. ***Comment****: There are many images in the article. Consider combining some of them for display.*

Response: Thank you for your suggestion. The article contains a substantial amount of content, resulting in a large number of images and tables, which has made the manuscript quite lengthy. Additionally, some figures provide limited information. Therefore, we have combined the Thiessen polygon results from Figure 5 into Figure 3, and merged the historical disaster point bar chart from Figure 6 with Figure 4. We also removed Figure 11, which depicted the rainfall forecast stations, as it did not present useful information. The revised content can be found in lines 136-137 and 147-149 (in red font).

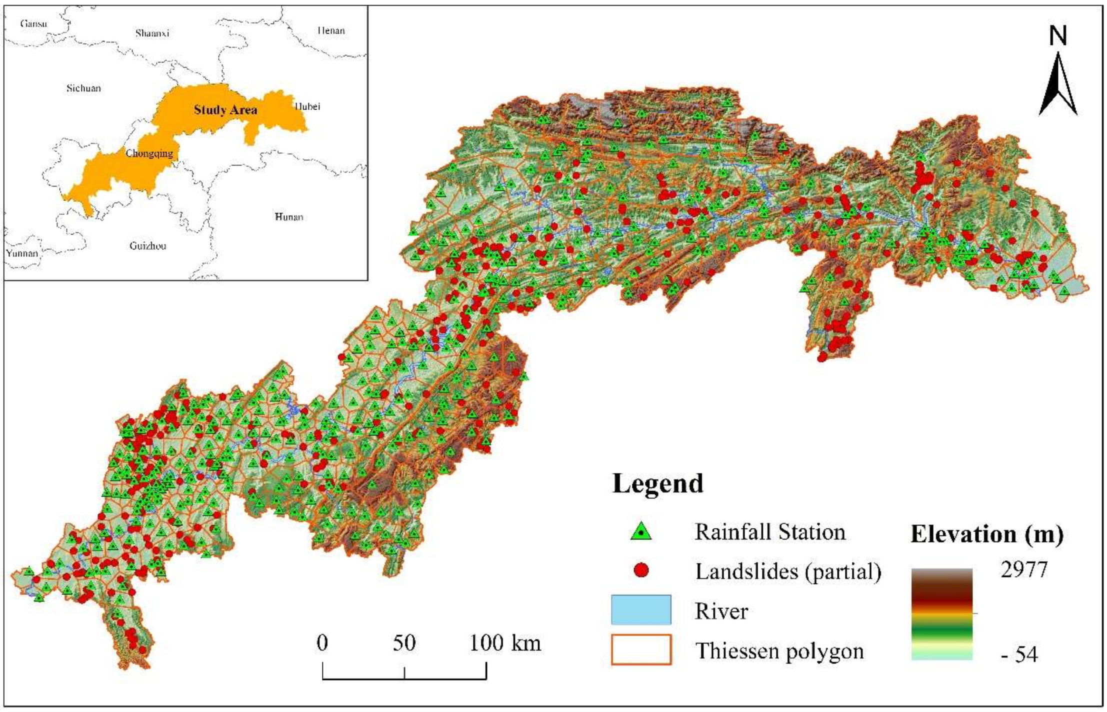

Figure 3: Geographic location of the study area and Thiessen polygon results of rainfall stations.

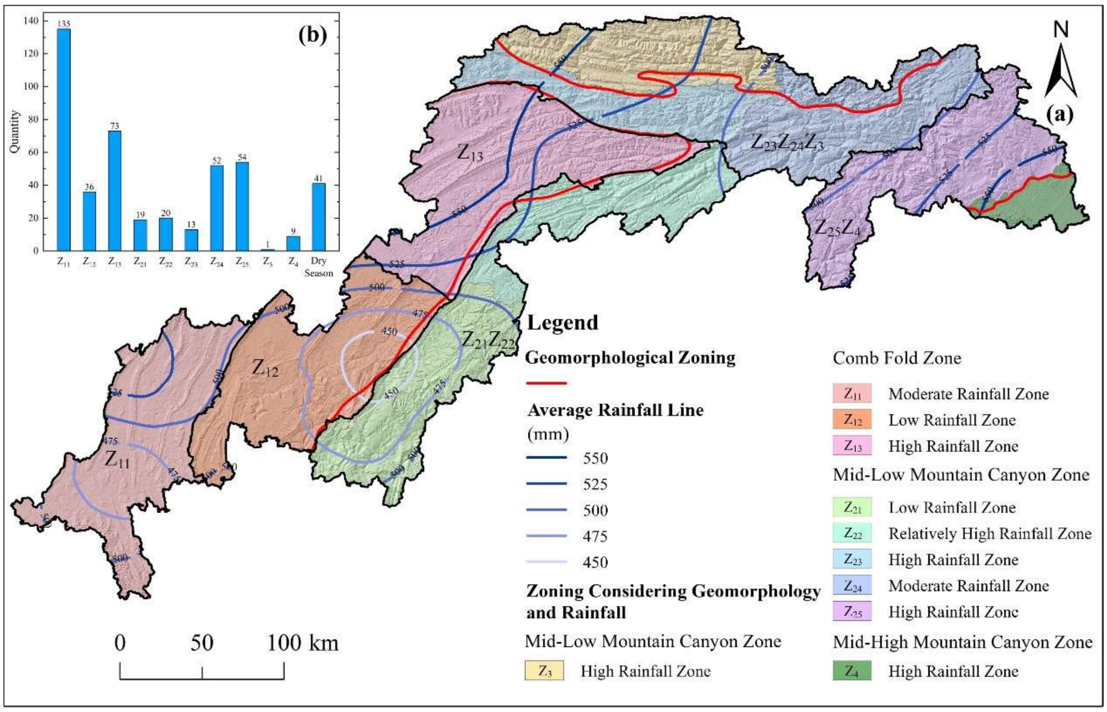

Figure 4: Zoning map of the study area. (a) Schematic diagram of the sub-region merger; (b) The number of historical landslide hazard sites in each sub-region.

8. Comment*: Some descriptions of the figures, such as the explanation of different* *colors in Figure 9 in lines 223-224, should be moved from the main text to the figure captions.*

Response: Thank you for pointing this out. We apologize for placing some explanatory notes that should be in the figure or table captions within the main text, which has made the text unnecessarily lengthy. We have reviewed and revised the captions for all figures and tables accordingly. The affected figures and tables include Figure 6 (formerly Figure 8), Figure 7 (formerly Figure 9), Table 9, Figure 14 (formerly Figure 17), and Figure 16 (formerly Figure 19). The revised content can be found in lines 204-208, 220-223, 318-319, 329-332, and 353-356 (in red font).

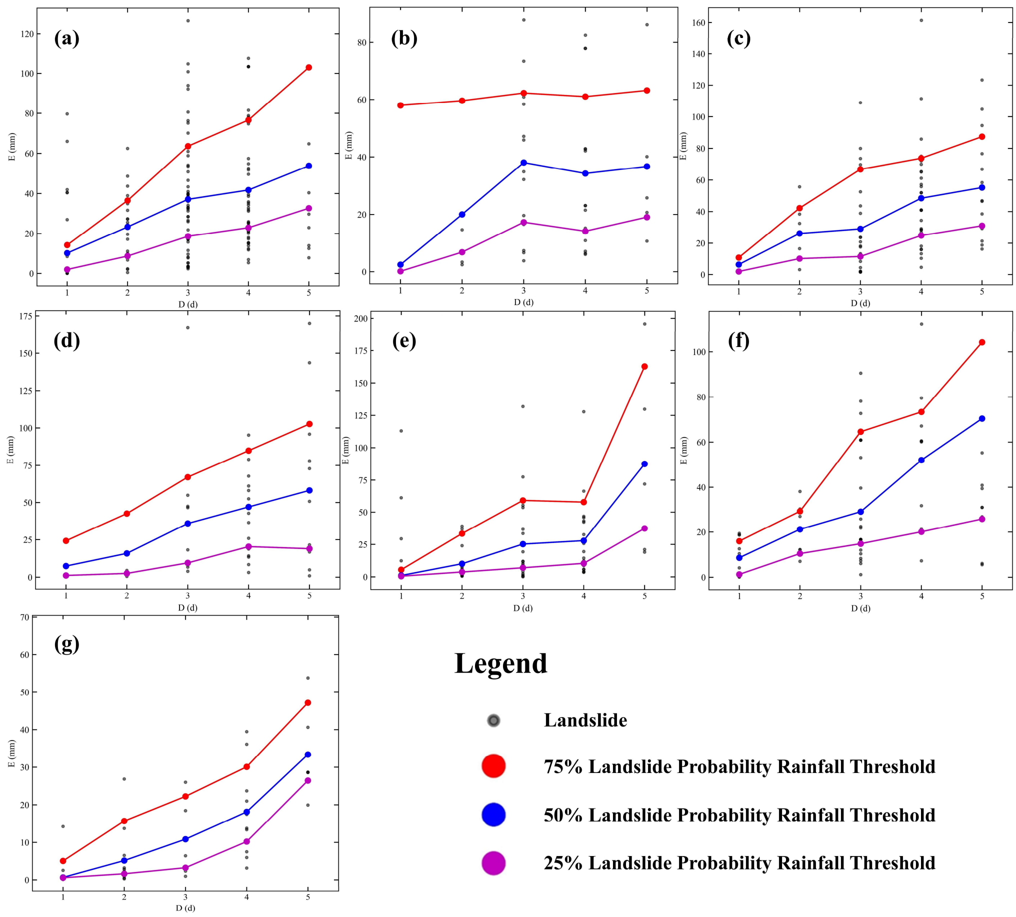

Figure 6: Plot of E-D rainfall threshold model results (MLP regression). In the figure, a is the Z_{11} region, b is the Z_{12} region, c is the Z_{13} region, d is the $Z_{21}Z_{22}$ region, e is the $Z_{23}Z_{24}Z_{3}$ region, f is the $Z_{25}Z_{4}$ region, and g is

the Dry Season. The red, blue and purple points in the figure are the rainfall threshold points obtained by fitting different landslide probabilities. The line segments are only used to connect the threshold points for viewing and have no practical significance.

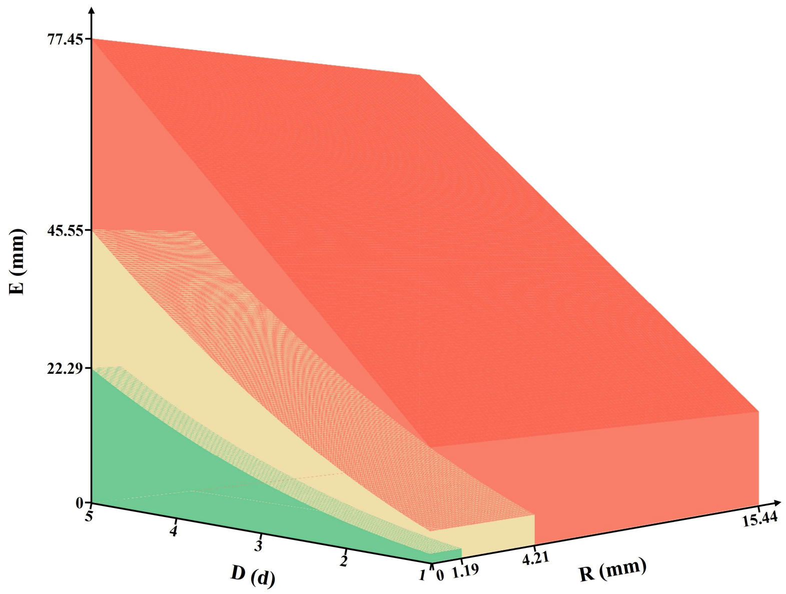

Figure 7: Schematic diagram of the E-D-R rainfall threshold model in Z13 region obtained by OLS regression. The green, yellow and red boxes in the figure represent the landslide probability when the rainfall threshold is <25%, 25-50% and 50-75%, respectively.

Table 9: Landslide susceptibility and rainfall warning level superposition matrix. In the table, 1 indicates relatively stable zone, 2 indicates general prevention zone, 3 indicates secondary prevention zone, and 4 indicates priority prevention zone.

Rainfall Threshold Level \ Susceptibility	Very Low	Low	Moderate	High	Very High
Caution	1	1	1	1	2
Special Caution	1	1	1	2	3
Warning	1	1	2	3	4
Severe Warning	1	2	3	4	4

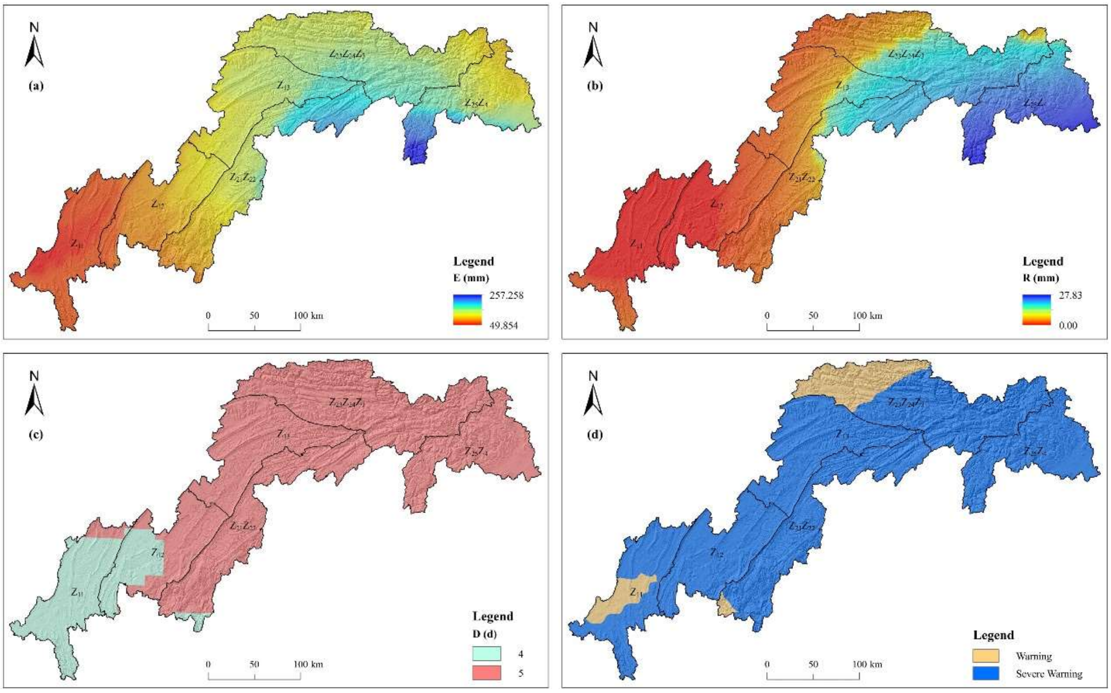

Figure 14: Various rainfall parameters and rainfall warning levels on July 19, 2020. (a) Effective rainfall obtained by Kriging interpolation; (b) Rainfall for the day obtained by Kriging interpolation; (c) Duration of rainfall obtained by Thiessen polygons; (d) Rainfall warning level calculated by the optimal rainfall threshold model.

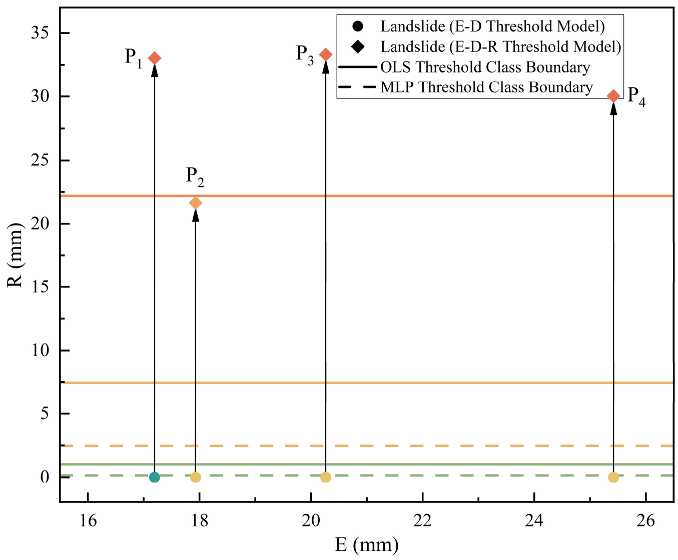

Figure 16: Rainfall warning level transition process (Z_{12} region). Green is the dividing line between Special Attention and Attention levels; yellow is the dividing line between Warning and Special Attention levels; orange is the dividing line between Severe Warning and Warning levels.

9. Comment*: The clarity of Figure 14 is insufficient. It is recommended to change* *the layout from three columns to two columns.*

Response: Thank you for bringing this to our attention. Following your suggestion, we have changed the layout of the figure from three columns to two columns to improve clarity. The revised content can be found in lines 296-297 (in red font).

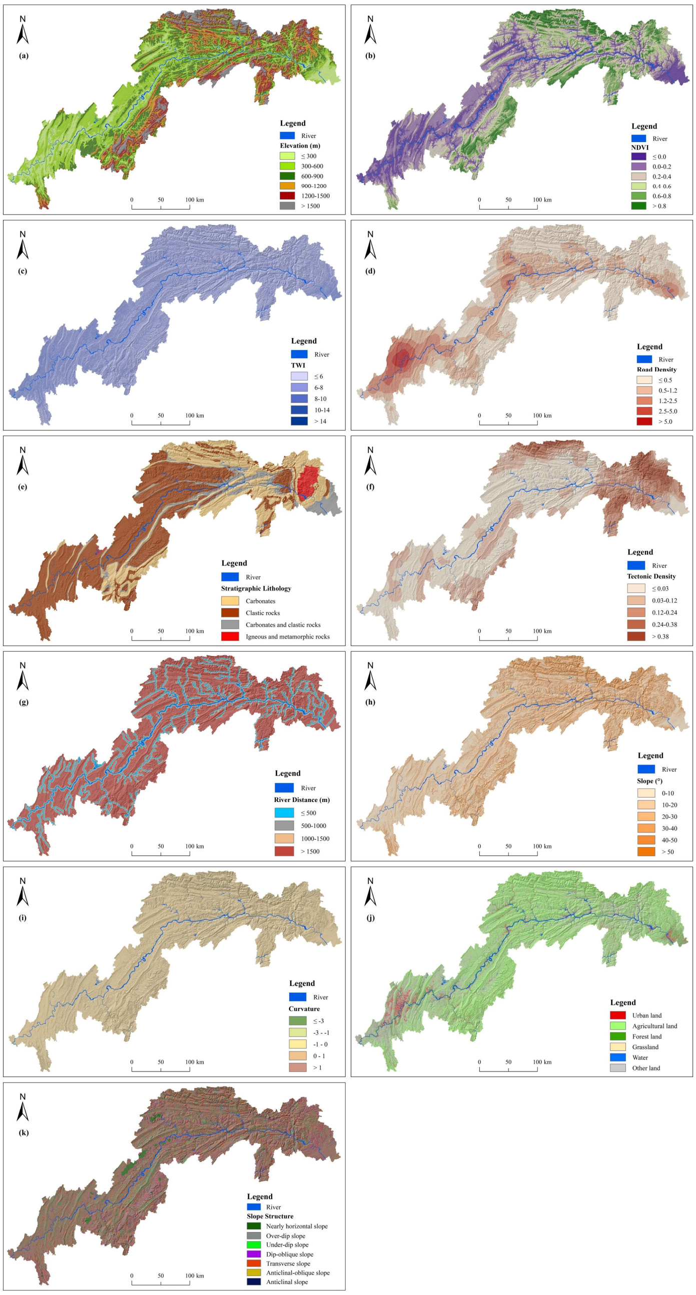

Figure 11: Landslide inducing factors grading results map.

Special thanks to you for your insightful and valuable comments in detail.